JNC TN9400 2004-075

JNC-CEA GCFR CORE NEUTRONIC BENCHMARK

February, 2005

O-ARAI ENGINEERING CENTER

JAPAN NUCLEAR CYCLE DEVELOPMENT INSTITUTE

JNC TN9400 2004-075
February, 2005

JNC-CEA GCFR CORE NEUTRONIC BENCHMARK

Kazuteru SUGINO[*1], Gerald RIMPAULT[*2],
Hideyuki HAYASHI[*3]

ABSTRACT

Within the NWP-2 (Innovative core and plant design) of the JNC/CEA bilateral agreement, it was decided to perform GCFR neutronic benchmarks in order to verify the adequacy of computational tools for the definition of GCFR core characteristics. The benchmarks have been performed on two different cores:

- A conventional CO_2-Cooled fast Reactor (EGCR) core with pin-type fuel
- An innovative He-cooled Coated-Particle Fuel (CPF) core

Results of the core design characteristics calculated by both JNC and CEA sides agreed quite satisfactorily and it is found that the remaining discrepancies do not influence the core conceptual design specification. Therefore these benchmark results can be used for ensuring some confidence in the GCFR core conceptual designs of both JNC and CEA.

For the improvement in the GCFR computational tools, this benchmark has been pointing out some issues. These issues are worth being investigated for improving the design accuracy of GCFR cores.

*1: Fuel and Core System Engineering Group, System Engineering Technology Division, O-arai Engineering Center, JNC, Japan
*2: Commissariat a l'Energie Atomique (CEA), France
*3: System Engineering Technology Division, O-arai Engineering Center, JNC, Japan (Present affiliation: Japan Atomic Energy Research Institute (JAERI), Japan)

JNC TN9400 2004-075
2005 年 2 月

JNC-CEA ガス冷却高速炉核特性ベンチマーク

（研究報告）

杉野 和輝[*1]、Gerald Rimpault [*2]、
林 秀行[*3]

要　旨

JNC-CEA 先進的技術協力の一環である「革新的な炉心およびプラント設計（NWP-2）」において、ガス冷却高速炉設計への炉心特性解析システムの適合性を評価するために、ガス冷却高速炉核特性ベンチマークの実施が合意された。ベンチマークは以下の異なる 2 種類の炉心に対して行なった。

・典型的な炭酸ガス冷却ピン型燃料炉心
・革新的なヘリウムガス冷却被覆粒子型燃料炉心

ベンチマークの結果、JNC と CEA の計算結果は良い一致を示し、双方の計算結果の差異による概念設計への影響は非常に小さいことが分かった。このように、本ベンチマークを通じて、JNC と CEA 双方のガス冷却高速炉の概念設計技術の信頼性向上を図ることができた。

また、本ベンチマークよりガス冷却高速炉の炉心解析における課題を抽出した。それらの課題の検討は、ガス冷却高速炉炉心の設計精度向上に非常に有用である。

*1: システム技術開発部　炉心・燃料システムグループ
*2: フランス原子力庁
*3: システム技術開発部（現、日本原子力研究所）

CONTENTS

LIST OF TABLES

LIST OF FIGURES

1. INTRODUCTION

The Gas-Cooled Fast Reactor (GCFR) neutronic benchmark has been performed by Japan Nuclear Cycle Development Institute (JNC) and Commissariat à l'Energie Atomique (CEA) as the joint studies defined in New Work Package (NWP)-2 (Innovative core and plant design) of the bilateral agreement. This benchmark is aiming at investigating the cross-evaluation of GCFR concepts by checking core neutronic characteristics using the core design tools of each organization. This will help clarifying the future issues associated to the improvement of the core designs with more reliable and accurate tools.

In the joint benchmark, two exercises were decided, that is, the standard pin-type core as the conventional one and the particle-fuel type core as the innovative one. For the benchmark, the GCFR cores developed in the feasibility study on the commercialized fast reactor cycle systems in Japan(1) have been selected. One is the Enhanced Gas-Cooled fast Reactor (EGCR) core(2) as the conventional type and another is the He-cooled Coated-Particle Fuel (CPF) core(3) as the innovative type.

Both JNC and CEA sides calculated the benchmark items using their own design tools and performed cross-comparison of several core parameters such as criticality, breeding gain, coolant depressurization reactivity, Doppler effect, burnup property.

2. SPECIFICATION OF THE GCFR CORE

Table 2.1-1 represents the basic specification of the conventional and innovative GCFR cores for the neutronic benchmark. The EGCR of the conventional type has CO_2-cooled pin-type oxide-fuel core. Core arrangement and fuel subassembly configuration of the EGCR core are shown in Fig. 2.1-1 and 2.1-2, respectively. As shown in Fig. 2.1-2 the basic structure of fuel subassembly is conventional like a sodium-cooled reactor core. The particle-fuel core of the innovative type has He-cooled TiN-coated-particle nitride-fuel (CPF) core. Core arrangement and fuel subassembly configuration of the CPF core are shown in Fig. 2.1-3, 2.1-4 and 2.1-5. The fuel subassembly of fuel part consists of inner and outer frits, fuel compartment and subassembly supporter. Coated-particle fuel is packed in the compartment formed by inner and outer frits. Coolant enters from the inner frit, passes horizontally through the compartment cooling the fuels, and exits outside the outer frit.

Detailed data for benchmark calculation such as dimensions and composition data are described in APPENDIX.

Table 2.1-1 Main specifications of two GCFRs - EGCR and CPF cores -

Items	Units	EGCR core (Conventional type)	Particle-fuel core (Innovative type)
Thermal output	MWth	3,600	2,400
Electric output	MWe	1,370	1,120
Outlet/Inlet temperatures	°C	530/266	850/460
Coolant type	-	Carbon dioxide (CO_2)	Helium (He)
Primary loop coolant pressure	MPa	4.2	6
Cycle operation length	EFPD	730	570
Refueling batch	Number	5	7
Fuel type	-	Sealed pin	Coated particle
Fuel material	-	Oxide	Nitride*1
Structural material	-	SS-316*2	SiC fiber/SiC composite
Core height	m	1.2	1.8
Blanket height	m	0.4 (Lower and Upper)	0.4 (Lower and Upper)
Fuel volume fraction	%	30.5	16.2
S/A pitch	mm	221.57	222.3
Core equivalent diameter	m	5.9	5.6
Envelope diameter of shielding region	m	8.7*3	7.5
Pu enrichment (IC/OC)	wt%	19.8/28.0	17.1/22.6
Burnup reactivity loss	%Δk/kk'	2.7	0.34
Breeding ratio	-	1.20	1.21
Fast neutron dose (E>0.1MeV)	n/cm^2	5.1×10^{23}	2.7×10^{23}
Core average discharge burnup	GWd/t	155	96
Core Doppler coefficient [Tdk/dT] (EOEC)	-	-5.0×10^{-3}	-8.8×10^{-3}
Coolant depressurization reactivity (EOEC)	$	1.2	0.94
Average core power density	W/cc	101	48
Average core liner heat rate	W/cm	123	-

*1: 100%-enriched N-15

*2: PE16 is also the candidate.

*3: Reduced to 7.8m with 2-layer radial shield

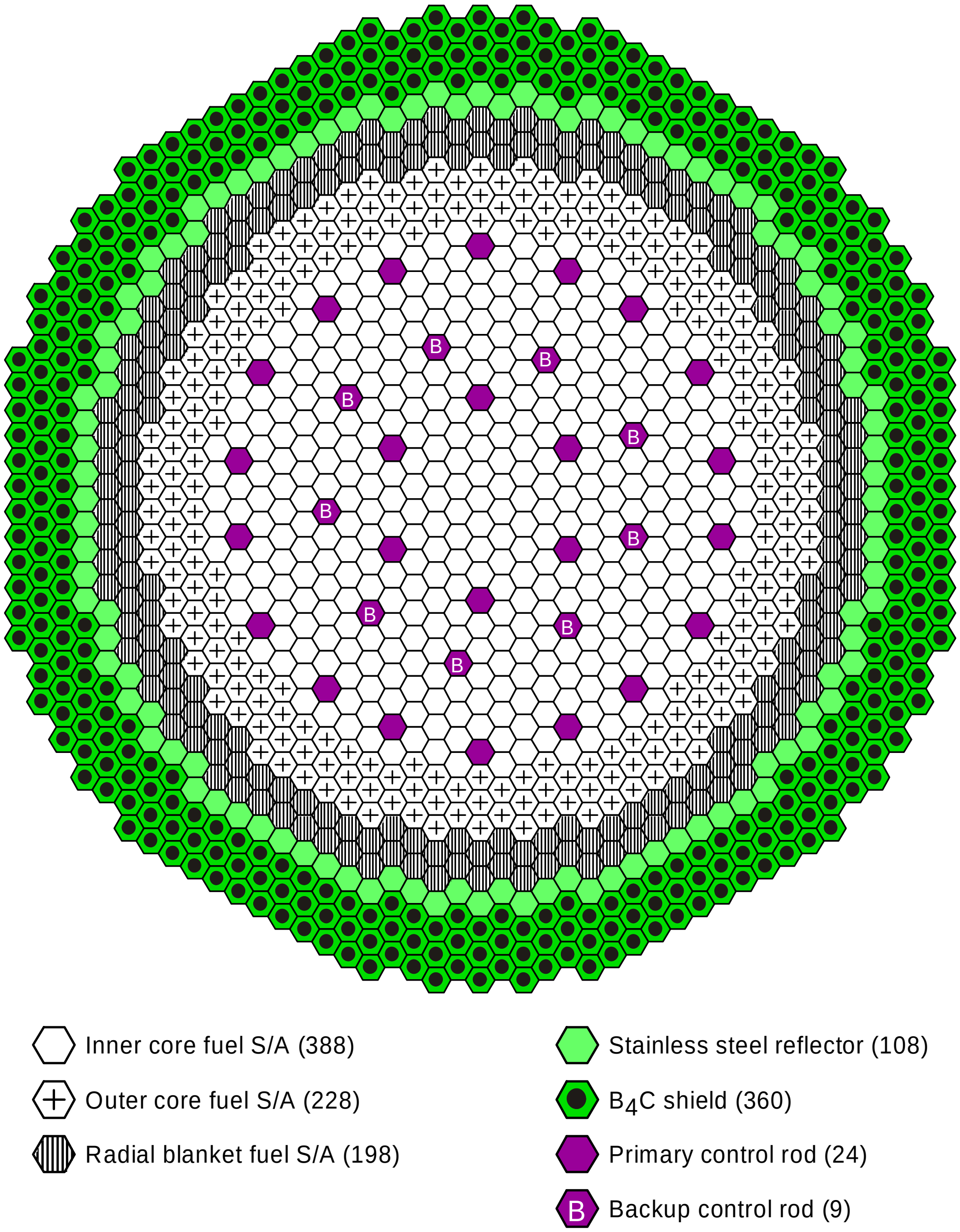

Fig. 2.1-1 Radial core layout - EGCR core -

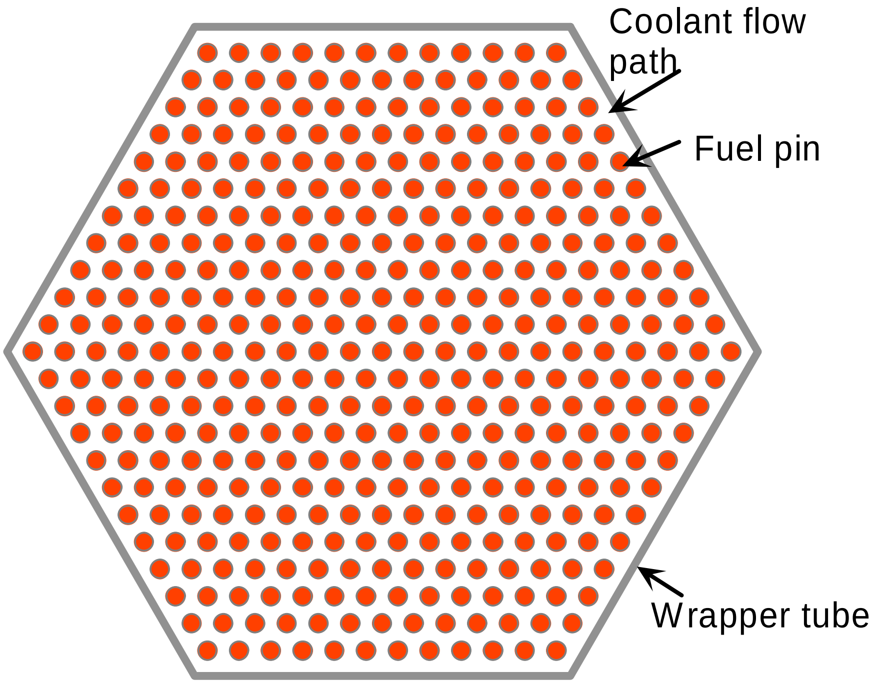

Fig. 2.1-2 Cross-sectional view of the subassembly - EGCR core -

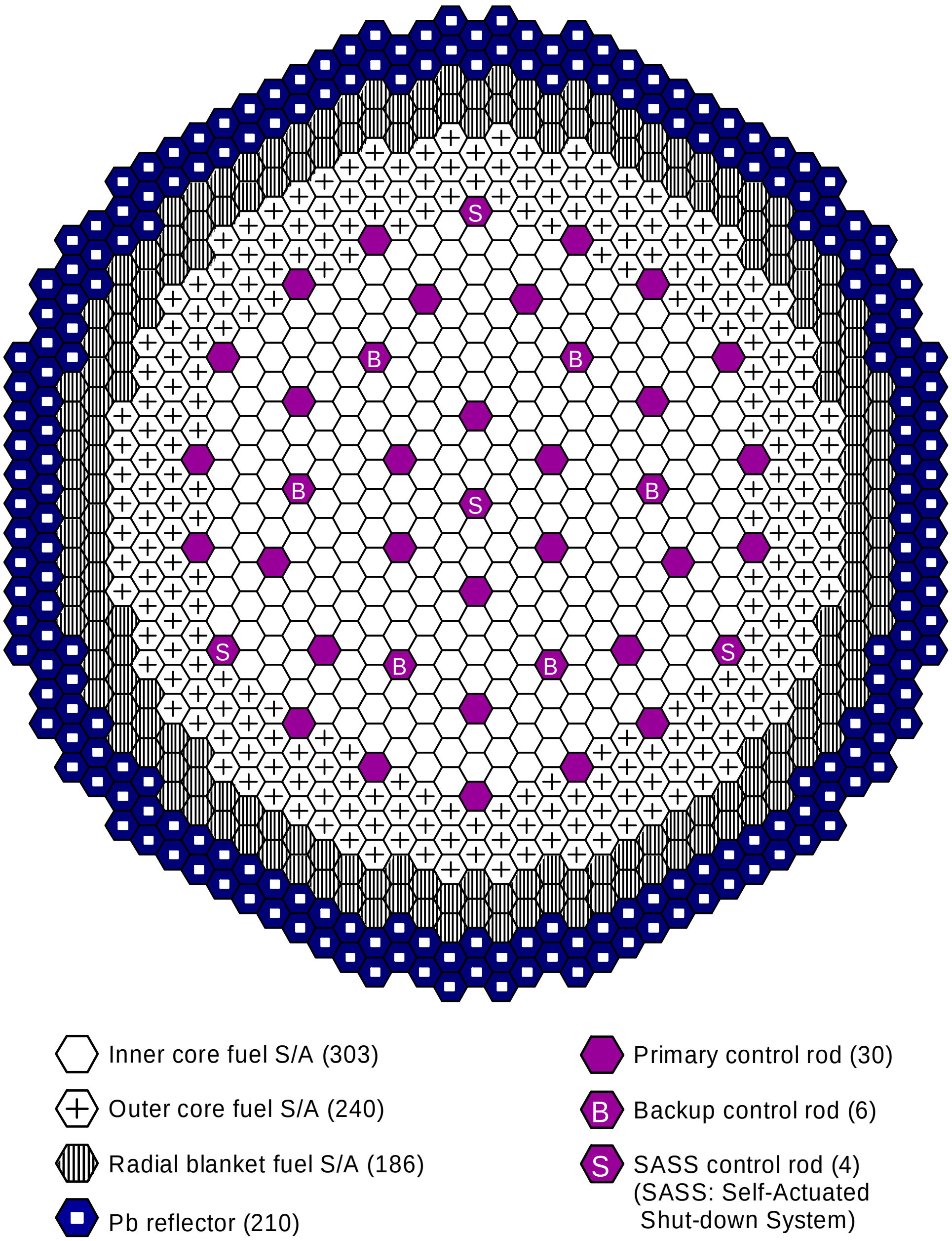

Fig. 2.1-3 Radial core layout - CPF core -

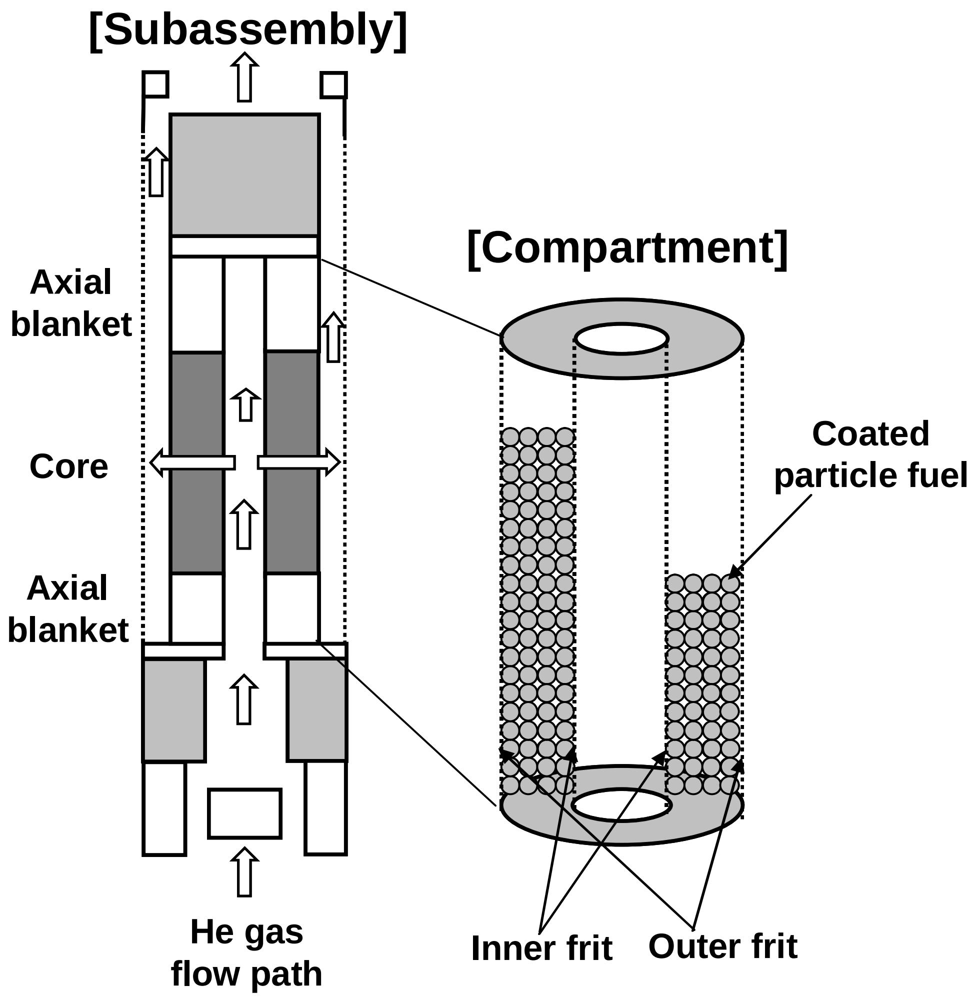

Fig. 2.1-4 Conceptual view of the fuel subassembly - CPF core -

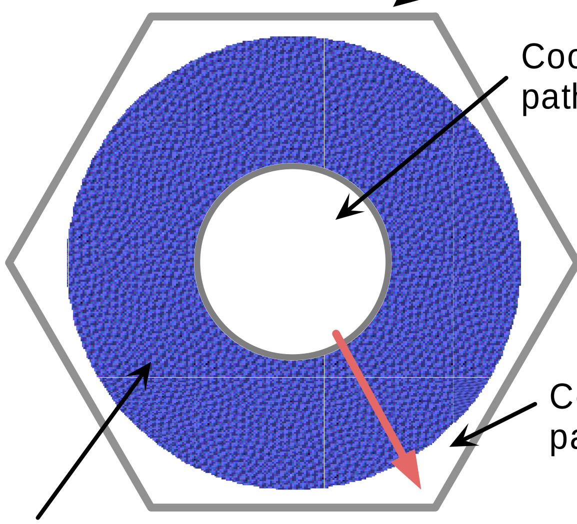

Fig. 2.1-5 Cross-sectional view of the subassembly - CPF core -

3. CALCULATION CONDITIONS AND METHODS

3.1 Calculation Conditions and Items

(1) Base Calculation Benchmark

In order to clarify the discrepancy of the analytical result derived from the difference of cross-section libraries, base calculation benchmark was carried out. Base calculation were performed using common geometry and composition.

a) Calculation conditions

As usual core design is performed based on the core parameters such as k-effective and coolant depressurization reactivity at EOEC (End Of Equilibrium Cycle) state for the conservative evaluation, the EOEC state was selected.

- Number densities: homogeneous cell model composition at EOEC
- 2D RZ core geometry
- Temperature of each region

Detailed data of above mentioned conditions are described in APPENDIX.

b) Calculation items

- Criticality (Effective multiplication factor)
- Instantaneous breeding gain (BG)
- Core Doppler effect
- Coolant depressurization reactivity

(2) Simple Depletion Calculation Benchmark

In order to check the influence due to the difference of depletion calculation systems, simple depletion calculation benchmark was performed.

a) Calculation conditions

- Number densities : homogeneous cell model composition of fresh fuel
- Depletion calculation for the initial cycle
  (Not equilibrium cycle)

Detailed data of above mentioned conditions are described in APPENDIX.

b) Calculation items

- Criticality at the beginning and the end of the initial cycle
- Burnup reactivity loss
- Mass balance of heavy metals and fission products (FP)

(3) Best Estimation Benchmark

For the comparison of the best estimated core parameters used in the core design study, best estimation benchmark was performed.

a) Calculation conditions

- Number densities : the composition of fresh fuel
- Heterogeneity cell description
- 2D RZ core geometry

Detailed data of above mentioned conditions are described in APPENDIX.

b) Calculation items

Heterogeneity effect, transport and mesh effect and best estimated values of following core parameters:

- Criticality
- Core Doppler effect
- Coolant depressurization reactivity

3.2 Calculation Methods

In the JNC side, adjusted cross-section library ADJ2000R(4) was applied, which was so called unified cross-sections because it unifies evaluated cross-section data and experimental data or differential and integral data. ADJ2000R was adjusted from JENDL-3.2 using 236 fast reactor core experiments. ADJ2000R has the 70-group structure. For the preparation of effective cross-section, table look-up method is used with self-shielding factor table(5). For the heterogeneity treatment of GCFR core fuel subassembly, Monte Carlo method(6) was adopted.

In the CEA side, adjusted cross-section library ERALIB1(7) was applied. ERALIB1 was prepared from JEF-2.2 using 75 fast and thermal reactor core experiments. ERALIB1 has several group structures and finest one has 1968-group structure. Effective cross-section is created by subgroup method with probability table(8). Heterogeneity of GCFR core fuel subassembly was treated by deterministic method(9).

Core neutron parameters were calculated in the usual way, however, unique treatments were adopted in the calculations of following core parameters.

(1) Instantaneous breeding gain

Instantaneous breeding gain BG is defined by following formula.

$$BG = \frac{\sum_n \left(C_n w_{n-capture} + D_n w_{n-decay}\right) - \sum_n \left(A_n + D_n\right) w_n}{\sum_n F_n} \tag{3-1}$$

Definitions of the variables used in the formula are as follows:

A_n : Absorption reaction rate of nuclide n, defined by $A_n = \int_{Core} d\mathbf{r} N_n(\mathbf{r}) \sigma_{a,n}(\mathbf{r}) \phi(\mathbf{r})$

F_n : Fission reaction rate of nuclide n, defined by $F_n = \int_{Core} d\mathbf{r} N_n(\mathbf{r}) \sigma_{f,n}(\mathbf{r}) \phi(\mathbf{r})$

C_n : Capture reaction rate of nuclide n, defined by $C_n = \int_{Core} d\mathbf{r} N_n(\mathbf{r}) \sigma_{c,n}(\mathbf{r}) \phi(\mathbf{r})$

D_n : Decay rate of nuclide n, defined by $D_n = \int_{Core} d\mathbf{r} \lambda_n N_n(\mathbf{r})$

σ_n^+ : Equivalent fissile cross-section averaged in the core region, defined by

$$\sigma_n^+ = \nu \sigma_{f,n} - \sigma_{a,n}$$

w_n : Core averaged reactivity weight or equivalent fissile coefficient of nuclide n, defined by

$$w_n = \frac{\sigma_n^+ - \sigma_{U-238}^+}{\sigma_{Pu-239}^+ - \sigma_{U-238}^+}$$

$n - capture$: Nuclide produced by capture reaction

$n - decay$: Nuclide produced by decay

The relationship between original nuclides and produced nuclides by capture reaction and decay in calculation of the breeding gain is shown in Table 3.2-1.

$\mathbf{r}$: Point vector

$N_n(\mathbf{r})$: Number density of nuclide n at $\mathbf{r}$

$\sigma_{a,n}(\mathbf{r})$: Microscopic absorption cross-section of nuclide n at $\mathbf{r}$

$\sigma_{f,n}(\mathbf{r})$: Microscopic fission cross-section of nuclide n at $\mathbf{r}$

$\sigma_{c,n}(\mathbf{r})$: Microscopic capture cross-section of nuclide n at $\mathbf{r}$

$\phi(\mathbf{r})$: Neutron flux at $\mathbf{r}$

λ_n: Decay constant of nuclide n

In this document, the breeding gain contributions of core region and blanket region are defined as internal breeding gain (IBG) and external breeding gain (EBG), respectively.

(2) Core Doppler effect

In fast reactor cores the Doppler reactivity is well-presented by following formula:

$$\rho \propto \frac{1}{T} \tag{3-2}$$

Here ρ is Doppler reactivity and T is absolute temperature.

Under the formula (3-3) Doppler effect α is defined by next equation.

$$\alpha = \frac{\rho_H - \rho_{Ref.}}{\ln\left(T_H / T_{Ref.}\right)} \tag{3-3}$$

Suffices Ref. and H represent the normal and power-increased states, respectively. In this benchmark, temperature at power-increased state is given by adding 500K to that at normal state in the core region as shown in the next equation.

$$T_H = T_{Ref.} + 500 \tag{3-4}$$

(3) Coolant depressurization reactivity

In this benchmark, coolant is assumed to disappear completely or become into vacuum in the reactor at the coolant depressurized state.

In the calculation by JNC, special treatment was applied. The former study clarified that the diffusion approximation error of the coolant depressurization reactivity of GCFR cores was caused dominantly in the Control Rod Position (CRP)[10]. Figures 3.2-1 and 3.2-2 represent the comparison of the exact perturbation calculation results between diffusion and transport theory for the depressurization reactivity of the CPF core. For the non-leakage component results based on both theories showed good agreement, however, for the leakage component considerable transport error was observed in the CRP region. Therefore in the JNC's calculation, coolant gas except for the CRP region was cleared when coolant depressurized, that is, coolant gas of the CRP region was set constant in both normal and depressurized states.

Table 3.2-1 Comparison of the produced nuclides by capture reaction and decay in calculation of the breeding gain

Nuclides	JNC		CEA	
	Capture	Decay	Capture	Decay
U-234	(Not considered)		U-235	(Just decay)
U-235	U-236		U-236	(Just decay)
U-236	Np-237		Np-237	(Just decay)
U-238	Np-239		Np-239	(Just decay)
Np-237	Pu-238		Pu-238	(Just decay)
Np-239	Pu-240	Pu-239	Pu-240	Pu-239
Pu-238	Pu-239		Pu-239	U-234
Pu-239	Pu-240		Pu-240	U-235
Pu-240	Pu-241		Pu-241	U-236
Pu-241	Pu-242	Am-241	Pu-242	Am-241
Pu-242	Am-243		Am-243	U-238
Am-241	Cm-242 (80%) Am-242m (20%)		Am-242 (85%) Am-242m (15%)	Np-237
Am-242	(Not directly considered)		Am-243	Pu-242 (17%) Cm-242 (83%)
Am-242m	Am-243		Am-243	Pu-242 (17%) Cm-242 (83%)
Am-243	Cm-244		Cm-244	Np-239
Cm-242	Cm-243	Pu-238	Cm-243	Pu-238
Cm-243	Cm-244		Cm-244	Pu-239
Cm-244	Cm-245		Cm-245	Pu-240
Cm-245	(Just incineration)		Cm-246	Pu-241
Cm-246	(Not considered)		Cm-247	Pu-242
Cm-247	(Not considered)		Cm-248	Am-243
Cm-248	(Not considered)		(Just incineration)	(Just decay)

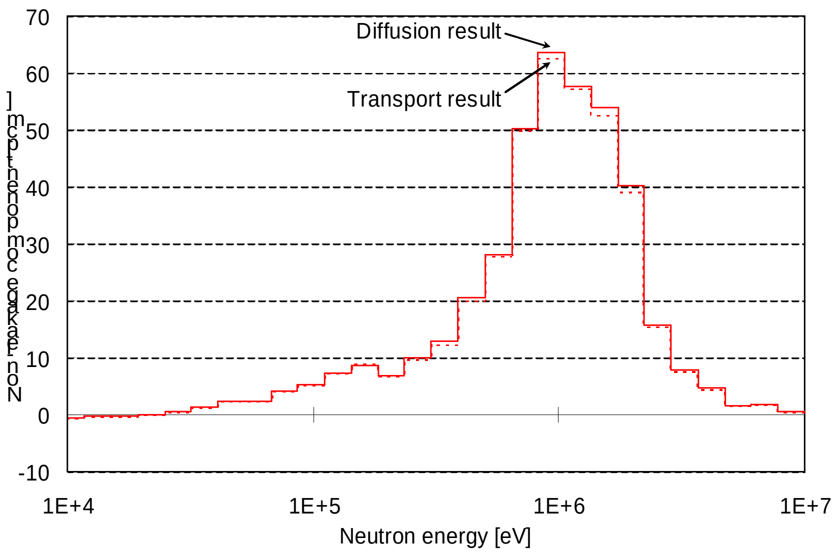

Fig. 3.2-1 Comparison of the diffusion and transport calculation for the non-leakage component of the depressurization reactivity of the CRP core

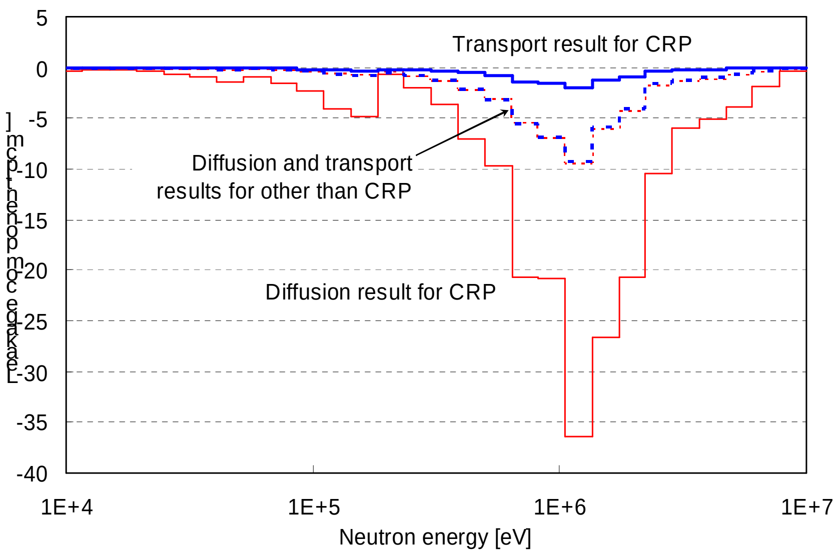

Fig. 3.2-2 Comparison of the diffusion and transport calculation for the leakage component of the depressurization reactivity of the CRP core

4. CALCULATION RESULTS

4.1 Base Calculation Benchmark Results

(1) Criticality, Core Doppler effect and Coolant depressurization reactivity

The results of the base calculation benchmark were shown in Table 4.1-1(1) and 4.1-1(2) for criticality, core Doppler effects and coolant depressurization reactivity of EGCR and CPF cores. CEA underestimated criticality by 0.6 through 1.5%Δk compared with JNC's results. These discrepancies are quite large in terms of the nuclear design. Now we consider these discrepancies in terms of the conceptual core design study. Table 4.1-2 represents the sensitivity factors of criticality for the EGCR and CPF cores. This table shows that the increase of the Pu-enrichment by 1wt% causes that of criticality by around 3%Δk for the both EGCR and CPF cores. That means that discrepancies in criticality correspond up to the difference of Pu-enrichment by 0.5wt%, which corresponds to the level of fabrication allowance. Therefore it is judged that discrepancies in criticality do not influence the core conceptual design specifications due to the difference of the core design tools.

For Doppler effect and coolant depressurization reactivity, good agreement was observed.

(2) Instantaneous breeding gain

Table 4.1-3 shows the comparison of the reactivity weights between CEA and JNC sides. The discrepancy arises mainly from that of the nuclear data, however, there is no large discrepancy. The results of the instantaneous breeding gain are shown in Table 4.1-4(1) for the EGCR core and in Table 4.1-4(2) for the CPF core, respectively. It is found that a lot of cancellation results in the little discrepancy in total breeding gain, and they agreed within 0.02. It is considered that discrepancies in components are mainly due to the difference in the nuclear data and such a related property as neutron flux distribution.

4.2 Simple Depletion Calculation Benchmark Results

(1) Criticality and burnup reactivity loss

Tables 4.2-1(1) and 4.2-1(2) represent the results of the k-effective and burnup reactivity loss by depletion over one cycle. The discrepancies in criticality are smaller than those observed in the base benchmark calculation, where more FPs are included in the fuel. Therefore absorption cross-section of the CEA's lumped FP would be larger than the JNC's one, and that resulted in the larger burnup reactivity loss.

(2) Mass balance

Tables 4.2-2(1) through 4.2-2(8) represent the results of the mass balance by JNC and absolute discrepancy between JNC and CEA for both GCFR cores. There is no large discrepancy in the heavy metal mass balance. However, the amount of FPs produced by CEA calculation is less important than JNC one. It is thought to be due to differences on many burn up parameters such as the lumped FP weight, energy release per fission and treatment of the heat generation by non-fuel nuclides.

4.3 Best Estimation Benchmark Results

(1) Criticality

Tables 4.3-1(1) and 4.3-1(2) represent the results of corrections and best estimated parameters for K-effective. For the EGCR core, there is no significant discrepancy in corrections. For the CPF core, considerable discrepancy is observed in transport and mesh effect, and the approach for the solution should be investigated. Discrepancies of best estimated values or corrected ones are not large in terms of the core conceptual design study.

(2) Core Doppler effect
Tables 4.3-2(1) and 4.3-2(2) represent the results of corrections and best estimated parameters for core Doppler effect. There is no significant discrepancy in corrections and best estimated values.

(3) Coolant depressurization reactivity
Tables 4.3-3(1) and 4.3-3(2) represent the results of corrections and best estimated parameters for coolant depressurization reactivity. There is no significant discrepancy in corrections and best estimated values.

4.4 Summary

(1) Criticality
Criticalities calculated by JNC and CEA agreed satisfactorily in terms of the core conceptual design study. For the improvement of the core design accuracy, further investigations are required particularly on the lumped FP cross-sections (and related burn up parameters) for any core designs and heterogeneity effect, transport and mesh effects for the GCFR core designs.

(2) Core Doppler effect
The agreement between JNC's and CEA's results were within 6%, and further investigation is not required.

(3) Coolant depressurization reactivity
The agreement between JNC's and CEA's results were within 0.2$, and further investigation is not required.

(4) Instantaneous breeding gain (BG)
The agreement in total BG was within 0.02 between JNC's and CEA's results for both EGCR and CPF cores.

(5) Burnup reactivity loss
The discrepancy is not large and investigation in lumped FP cross-sections will improve the agreement.

(6) Mass balance by depletion calculation
Good agreement was obtained on the heavy nuclide mass balance. Concerning the FP, many parameters (lumped FP weight, energy release per fission and treatment of the heat generation by non-fuel nuclides) contribute with their discrepancies to the mass differences between JNC and CEA.

Table 4.1-1(1) Comparison of the base calculation benchmark results - EGCR core -

Items	JNC	CEA	Discrepancy*1
Criticality	0.99378	0.97873	-0.01505
Core Doppler effect [10^{-3}Tdk/dT]	-3.55	-3.34	+0.21
Coolant depressurization reactivity [$]	+1.18	+1.31	+0.13

*1: Reference is result by JNC βeff=0.00355

Table 4.1-1(2) Comparison of the base calculation benchmark results - CPF core -

Items	JNC	CEA	Discrepancy*1
Criticality	0.98305	0.97725	-0.00579
Core Doppler effect [10^{-3}Tdk/dT]	-9.74	-9.93	-0.19
Coolant depressurization reactivity [$]	+1.28	+1.01	-0.27

*1: Reference is result by JNC βeff=0.00331

Table 4.1-2 Sensitivity coefficients for criticality - EGCR and CPF cores -

Elements	EGCR core	CPF core
U	0.00169	0.00233
Pu	0.02418	0.02633
MA	0.00017	0.00001
Total	0.02604	0.02868

Unit: Δk/(Pu-enrichment [wt%])

Table 4.1-3 Comparison of the reactivity weights - EGCR and CPF cores -

Nuclides	EGCR core		CPF core		
	JNC	CEA	JNC	CEA	
U-234	-	0.02	-	-0.06	
U-235	0.73	0.77	0.82	0.75	
U-236	-0.01	-0.06	-0.04	-0.09	
U-238	0.00	0.00	0.00	0.00	Fixed
Np-237	-0.19	-0.27	-0.33	-0.42	
Np-239	-0.20	-0.31	-0.41	-0.44	
Pu-238	0.60	0.57	0.54	0.40	
Pu-239	1.00	1.00	1.00	1.00	Fixed
Pu-240	0.17	0.11	0.12	-0.19	
Pu-241	1.43	1.47	1.60	1.51	
Pu-242	0.12	0.08	0.08	0.02	
Am-241	-0.19	-0.35	-0.33	-0.58	
Am-242	-	2.23	-	2.29	
Am-242m	2.05	2.18	2.32	3.13	
Am-243	-0.19	-0.33	-0.30	-0.42	
Cm-242	0.51	0.30	0.46	0.16	
Cm-243	2.20	2.51	2.59	2.43	
Cm-244	0.24	0.20	0.17	0.04	
Cm-245	1.99	2.42	2.28	2.58	
Cm-246	-	0.22	-	0.16	
Cm-247	-	1.55	-	1.36	
Cm-248	-	0.24	-	0.16	

Table 4.1-4(1) Comparison of the breeding gain in the base calculation benchmark - EGCR core -

Nuclides	JNC			CEA			Discrepancy[*1]		
	IBG	EBG	TBG	IBG	EBG	TBG	IBG	EBG	TBG
U-235	-0.006	-0.007	-0.013	-0.007	-0.008	-0.014	-0.001	-0.000	-0.001
U-236	-0.000	-0.000	-0.000	-0.000	-0.000	-0.000	-0.000	-0.000	-0.000
U-238	-0.113	-0.094	-0.207	-0.183	-0.142	-0.325	-0.070	-0.048	-0.118
Np-237	+0.004	+0.000	+0.004	+0.004	+0.000	+0.004	+0.000	+0.000	+0.000
Np-239	+0.639	+0.545	+1.184	+0.760	+0.588	+1.348	+0.121	+0.043	+0.164
Pu-238	-0.004	-0.000	-0.004	-0.005	-0.000	-0.005	-0.001	-0.000	-0.001
Pu-239	-0.686	-0.101	-0.787	-0.710	-0.105	-0.815	-0.024	-0.004	-0.027
Pu-240	+0.121	+0.002	+0.124	+0.131	+0.003	+0.134	+0.010	+0.000	+0.010
Pu-241	-0.163	-0.001	-0.164	-0.174	-0.001	-0.175	-0.011	-0.000	-0.011
Pu-242	-0.004	-0.000	-0.004	-0.005	+0.000	-0.005	-0.000	+0.000	-0.000
Am-241	+0.023	+0.000	+0.023	+0.069	+0.000	+0.069	+0.046	+0.000	+0.046
Am-242	-	-	-	-0.044	-0.000	-0.044	-0.044	-0.000	-0.044
Am-242m	-0.006	-0.000	-0.006	-0.006	+0.000	-0.006	-0.001	+0.000	-0.001
Am-243	+0.005	+0.000	+0.005	+0.006	+0.000	+0.006	+0.002	-0.000	+0.002
Cm-242	+0.002	+0.000	+0.002	+0.005	+0.000	+0.005	+0.003	+0.000	+0.003
Cm-243	-0.000	-0.000	-0.000	+0.007	+0.000	+0.007	+0.008	+0.000	+0.008
Cm-244	+0.007	+0.000	+0.007	-0.000	+0.000	-0.000	-0.008	-0.000	-0.008
Cm-245	-0.005	-0.000	-0.005	-0.006	+0.000	-0.006	-0.001	+0.000	-0.001
Total	-0.187	+0.345	+0.158	-0.158	+0.336	+0.178	+0.029	-0.009	+0.020

*1: Reference is result by JNC

Table 4.1-4(2) Comparison of the breeding gain in the base calculation benchmark - CPF core -

Nuclides	JNC			CEA			Discrepancy[*1]		
	IBG	EBG	TBG	IBG	EBG	TBG	IBG	EBG	TBG
U-235	-0.009	-0.011	-0.020	-0.009	-0.012	-0.021	+0.000	-0.001	-0.001
U-236	-0.000	-0.000	-0.000	-0.000	-0.000	-0.000	-0.000	-0.000	-0.000
U-238	-0.272	-0.202	-0.473	-0.312	-0.253	-0.565	-0.040	-0.051	-0.092
Np-237	+0.004	+0.000	+0.005	+0.004	+0.000	+0.005	-0.000	+0.000	-0.000
Np-239	+0.944	+0.671	+1.616	+0.983	+0.797	+1.779	+0.038	+0.125	+0.164
Pu-238	-0.002	+0.000	-0.002	-0.001	+0.000	-0.001	+0.001	+0.000	+0.001
Pu-239	-0.729	-0.161	-0.890	-0.801	-0.179	-0.979	-0.071	-0.018	-0.089
Pu-240	+0.172	+0.014	+0.186	+0.214	+0.015	+0.229	+0.041	+0.001	+0.043
Pu-241	-0.208	-0.010	-0.218	-0.217	-0.010	-0.227	-0.008	-0.000	-0.009
Pu-242	-0.005	-0.000	-0.005	-0.005	-0.000	-0.005	+0.000	+0.000	+0.000
Am-241	+0.032	+0.000	+0.033	+0.092	+0.001	+0.094	+0.060	+0.001	+0.061
Am-242	-	-	-	-0.054	-0.001	-0.055	-0.054	-0.001	-0.055
Am-242m	-0.006	-0.000	-0.006	-0.009	-0.000	-0.009	-0.003	-0.000	-0.003
Am-243	+0.005	+0.000	+0.005	+0.006	+0.000	+0.006	+0.001	-0.000	+0.001
Cm-242	+0.002	+0.000	+0.002	+0.006	+0.000	+0.006	+0.004	+0.000	+0.004
Cm-243	-0.000	-0.000	-0.000	+0.008	+0.000	+0.008	+0.009	+0.000	+0.009
Cm-244	+0.010	+0.000	+0.010	-0.000	+0.000	-0.000	-0.010	-0.000	-0.010
Cm-245	-0.005	-0.000	-0.005	-0.006	+0.000	-0.006	-0.001	+0.000	-0.001
Total	-0.067	+0.303	+0.236	-0.102	+0.359	+0.257	-0.035	+0.056	+0.021

*1: Reference is result by JNC

Table 4.2-1(1) Comparison of the burnup reactivity loss in the simple depletion calculation benchmark - EGCR core -

Items	JNC	CEA	Discrepancy*1
Keff at BOC	1.09101	1.08462	-0.00639
Keff at EOC	1.05071	1.04326	-0.00745
Burnup reactivity loss [%Δk/kk']	+3.52	+3.66	+0.14

*1: Reference is result by JNC

Table 4.2-1(2) Comparison of the burnup reactivity loss in the simple depletion calculation benchmark - CPF core -

Items	JNC	CEA	Discrepancy*1
Keff at BOC	0.99546	0.99752	+0.00206
Keff at EOC	0.99547	0.99452	-0.00095
Burnup reactivity loss [%Δk/kk']	-0.00	+0.30	+0.30

*1: Reference is result by JNC

Table 4.2-2(1) Result of the mass balance in the core region by JNC - EGCR core -

Nuclides	Inner core			Outer core		
	BOC	EOC	Balance	BOC	EOC	Balance
U-235	112.1	89.5	-22.6	58.9	46.1	-12.8
U-236	0.0	4.7	4.7	0.0	2.6	2.6
U-238	37,251.0	36,127.8	-1,123.2	19,588.4	18,935.2	-653.2
Np-237	49.0	46.4	-2.6	40.8	37.5	-3.3
Np-239	0.0	4.5	4.5	0.0	2.4	2.4
Pu-238	107.6	112.3	4.7	89.7	92.3	2.6
Pu-239	5,291.1	5,100.0	-191.0	4,412.5	3,927.6	-485.0
Pu-240	3,139.4	3,094.4	-45.0	2,618.1	2,541.9	-76.3
Pu-241	420.5	418.6	-1.9	350.7	343.4	-7.3
Pu-242	381.4	372.3	-9.1	318.1	307.9	-10.2
Am-241	195.8	199.2	3.4	163.3	163.7	0.4
Am-242m	0.0	5.3	5.3	0.0	4.4	4.4
Am-243	97.9	98.7	0.8	81.6	81.7	0.1
Cm-242	0.0	7.6	7.6	0.0	6.2	6.2
Cm-243	0.0	0.2	0.2	0.0	0.2	0.2
Cm-244	97.9	101.0	3.1	81.6	83.3	1.7
Cm-245	0.0	5.4	5.4	0.0	4.6	4.6
Total FP*	0.0	1,378.0	1,378.0	0.0	1,259.4	1,259.4

Unit: kg

*: Excluded accompanying FP in low-DF reprocessing

Table 4.2-2(2) Absolute discrepancy of the mass balance in the core region between JNC and CEA - EGCR core -

Nuclides	Inner core			Outer core		
	BOC	EOC	Balance	BOC	EOC	Balance
U-235	-0.0	+1.4	+1.4	-0.0	-0.1	-0.1
U-236	+0.0	+0.6	+0.6	+0.0	+0.7	+0.7
U-238	-2.2	+56.4	+58.6	-1.1	-21.6	-20.5
Np-237	-0.0	+0.9	+1.0	-0.0	+0.7	+0.7
Np-239	+0.0	-0.4	-0.4	+0.0	+0.1	+0.1
Pu-238	-0.0	-0.6	-0.6	-0.0	-0.0	-0.0
Pu-239	-0.4	+25.9	+26.3	-0.3	+0.8	+1.1
Pu-240	-0.2	+29.9	+30.1	-0.2	+24.6	+24.7
Pu-241	-0.0	-9.6	-9.6	-0.0	-7.1	-7.1
Pu-242	-0.0	+6.8	+6.8	-0.0	+6.1	+6.1
Am-241	-0.0	-1.5	-1.5	-0.0	-4.4	-4.4
Am-242m	+0.0	-1.1	-1.1	+0.0	-0.7	-0.7
Am-243	-0.0	-2.8	-2.8	-0.0	-2.7	-2.7
Cm-242	+0.0	-0.7	-0.7	+0.0	+0.2	+0.2
Cm-243	+0.0	+0.0	+0.0	+0.0	+0.1	+0.1
Cm-244	-0.0	-5.3	-5.3	-0.0	-3.9	-3.9
Cm-245	+0.0	-1.5	-1.5	+0.0	-0.9	-0.9
Total FP*	+0.0	-131.1	-131.1	+0.0	-37.0	-37.0

Unit: kg

Remark: Reference of difference is result by JNC

*: Excluded accompanying FP in low-DF reprocessing

Table 4.2-2(3) Result of the mass balance in the blanket region by JNC - EGCR core -

Nuclides	Axial blanket			Radial blanket		
	BOC	EOC	Balance	BOC	EOC	Balance
U-235	169.3	152.0	-17.3	208.3	194.0	-14.3
U-236	0.0	4.1	4.1	0.0	3.5	3.5
U-238	56,274.6	55,546.7	-727.9	69,209.7	68,628.1	-581.6
Np-237	0.0	1.6	1.6	0.0	1.0	1.0
Np-239	0.0	3.2	3.2	0.0	2.5	2.5
Pu-238	0.0	0.1	0.1	0.0	0.0	0.0
Pu-239	0.0	642.9	642.9	0.0	525.8	525.8
Pu-240	0.0	11.0	11.0	0.0	7.3	7.3
Pu-241	0.0	0.2	0.2	0.0	0.1	0.1
Pu-242	0.0	0.0	0.0	0.0	0.0	0.0
Am-241	0.0	0.0	0.0	0.0	0.0	0.0
Am-242m	0.0	0.0	0.0	0.0	0.0	0.0
Am-243	0.0	0.0	0.0	0.0	0.0	0.0
Cm-242	0.0	0.0	0.0	0.0	0.0	0.0
Cm-243	0.0	0.0	0.0	0.0	0.0	0.0
Cm-244	0.0	0.0	0.0	0.0	0.0	0.0
Cm-245	0.0	0.0	0.0	0.0	0.0	0.0
Total FP	0.0	73.4	73.4	0.0	50.5	50.5

Unit: kg

Table 4.2-2(4) Absolute discrepancy of the mass balance in the blanket region between JNC and CEA - EGCR core -

Nuclides	Axial blanket			Radial blanket		
	BOC	EOC	Balance	BOC	EOC	Balance
U-235	-0.0	+0.1	+0.2	+0.0	+1.2	+1.2
U-236	+0.0	+0.2	+0.2	+0.0	-0.2	-0.2
U-238	-3.8	+33.7	+37.5	+2.5	+54.1	+51.6
Np-237	+0.0	-0.2	-0.2	+0.0	-0.1	-0.1
Np-239	+0.0	-0.2	-0.2	+0.0	-0.2	-0.2
Pu-238	+0.0	+0.0	+0.0	+0.0	+0.0	+0.0
Pu-239	+0.0	-35.0	-35.0	+0.0	-48.9	-48.9
Pu-240	+0.0	+1.4	+1.4	+0.0	-0.7	-0.7
Pu-241	+0.0	+0.1	+0.1	+0.0	-0.0	-0.0
Pu-242	+0.0	+0.0	+0.0	+0.0	+0.0	+0.0
Am-241	+0.0	+0.0	+0.0	+0.0	-0.0	-0.0
Am-242m	+0.0	+0.0	+0.0	+0.0	+0.0	+0.0
Am-243	+0.0	+0.0	+0.0	+0.0	+0.0	+0.0
Cm-242	+0.0	+0.0	+0.0	+0.0	+0.0	+0.0
Cm-243	+0.0	+0.0	+0.0	+0.0	+0.0	+0.0
Cm-244	+0.0	+0.0	+0.0	+0.0	+0.0	+0.0
Cm-245	+0.0	+0.0	+0.0	+0.0	+0.0	+0.0
Total FP	+0.0	+6.5	+6.5	+0.0	+3.8	+3.8

Unit: kg

Remark: Reference of difference is result by JNC

Table 4.2-2(5) Result of the mass balance in the core region by JNC - CPF core -

Nuclides	Inner core			Outer core		
	BOC	EOC	Balance	BOC	EOC	Balance
U-235	116.1	99.2	-16.9	86.7	77.3	-9.4
U-236	0.0	3.8	3.8	0.0	2.1	2.1
U-238	38,588.6	37,809.0	-779.6	28,807.7	28,368.9	-438.8
Np-237	41.9	40.0	-2.0	44.1	42.2	-1.9
Np-239	0.0	4.0	4.0	0.0	2.1	2.1
Pu-238	92.2	96.4	4.1	97.0	99.8	2.8
Pu-239	4,536.3	4,533.9	-2.3	4,770.5	4,621.7	-148.8
Pu-240	2,691.5	2,709.3	17.8	2,830.5	2,831.5	1.0
Pu-241	360.5	370.8	10.2	379.2	376.4	-2.8
Pu-242	327.0	323.0	-4.1	343.9	340.0	-3.9
Am-241	167.7	171.4	3.7	176.4	186.3	9.9
Am-242m	0.0	3.8	3.8	0.0	2.9	2.9
Am-243	83.9	85.0	1.2	88.2	88.9	0.7
Cm-242	0.0	6.2	6.2	0.0	4.7	4.7
Cm-243	0.0	0.1	0.1	0.0	0.1	0.1
Cm-244	83.9	86.6	2.7	88.2	90.0	1.8
Cm-245	0.0	3.8	3.8	0.0	2.9	2.9
Total FP*	0.0	744.0	744.0	0.0	577.7	577.7

Unit: kg

*: Excluded accompanying FP in low-DF reprocessing

Table 4.2-2(6) Absolute discrepancy of the mass balance in the core region between JNC and CEA - CPF core -

Nuclides	Inner core			Outer core		
	BOC	EOC	Balance	BOC	EOC	Balance
U-235	+0.4	+1.0	+0.6	+0.3	-0.1	-0.4
U-236	+0.0	+0.6	+0.6	+0.0	+0.7	+0.7
U-238	+125.4	+169.8	+44.4	+93.6	+74.0	-19.6
Np-237	+0.1	+0.8	+0.7	+0.1	+0.7	+0.5
Np-239	+0.0	-0.1	-0.1	+0.0	+0.2	+0.2
Pu-238	+0.3	-0.9	-1.2	+0.3	-0.6	-1.0
Pu-239	+14.7	+14.3	-0.4	+15.4	+11.1	-4.3
Pu-240	+8.7	+23.8	+15.1	+9.2	+22.7	+13.5
Pu-241	+1.2	-3.2	-4.4	+1.2	-0.6	-1.8
Pu-242	+1.1	+4.5	+3.4	+1.1	+3.9	+2.8
Am-241	+1.7	+0.5	-1.2	+0.6	-1.5	-2.1
Am-242m	+0.0	-1.0	-1.0	+0.0	-0.5	-0.5
Am-243	+0.3	-1.2	-1.5	+0.3	-1.0	-1.3
Cm-242	+0.0	-0.7	-0.7	+0.0	-0.0	-0.1
Cm-243	+0.0	+0.0	+0.0	+0.0	+0.0	+0.0
Cm-244	+0.3	-3.2	-3.4	+0.3	-3.4	-3.7
Cm-245	+0.0	-1.1	-1.1	+0.0	-0.7	-0.7
Total FP*	+0.0	-55.2	-55.2	+0.0	+10.6	+10.6

Unit: kg

Remark: Reference of difference is result by JNC

*: Excluded accompanying FP in low-DF reprocessing

Table 4.2-2(7) Result of the mass balance in the blanket region by JNC - CPF core -

Nuclides	Axial blanket			Radial blanket		
	BOC	EOC	Balance	BOC	EOC	Balance
U-235	157.7	135.7	-22.0	212.0	199.0	-12.9
U-236	0.0	4.7	4.7	0.0	2.8	2.8
U-238	52,419.4	51,966.7	-452.7	70,452.4	70,158.0	-294.4
Np-237	0.0	0.9	0.9	0.0	0.5	0.5
Np-239	0.0	2.6	2.6	0.0	1.7	1.7
Pu-238	0.0	0.0	0.0	0.0	0.0	0.0
Pu-239	0.0	350.6	350.6	0.0	259.2	259.2
Pu-240	0.0	23.8	23.8	0.0	6.9	6.9
Pu-241	0.0	4.1	4.1	0.0	0.4	0.4
Pu-242	0.0	0.2	0.2	0.0	0.0	0.0
Am-241	0.0	0.1	0.1	0.0	0.0	0.0
Am-242m	0.0	0.0	0.0	0.0	0.0	0.0
Am-243	0.0	0.0	0.0	0.0	0.0	0.0
Cm-242	0.0	0.0	0.0	0.0	0.0	0.0
Cm-243	0.0	0.0	0.0	0.0	0.0	0.0
Cm-244	0.0	0.0	0.0	0.0	0.0	0.0
Cm-245	0.0	0.0	0.0	0.0	0.0	0.0
Total FP	0.0	62.5	62.5	0.0	30.9	30.9

Unit: kg

Table 4.2-2(8) Absolute discrepancy of the mass balance in the blanket region between JNC and CEA - CPF core -

Nuclides	Axial blanket			Radial blanket		
	BOC	EOC	Balance	BOC	EOC	Balance
U-235	-0.0	+2.9	+2.9	-0.0	+0.5	+0.5
U-236	+0.0	-0.0	-0.0	+0.0	+0.3	+0.3
U-238	-3.8	+22.2	+26.0	-4.9	-9.5	-4.6
Np-237	+0.0	-0.2	-0.2	+0.0	+0.0	+0.0
Np-239	+0.0	-0.1	-0.1	+0.0	+0.1	+0.1
Pu-238	+0.0	+0.0	+0.0	+0.0	-0.0	-0.0
Pu-239	+0.0	-6.5	-6.5	+0.0	-0.3	-0.3
Pu-240	+0.0	-2.3	-2.3	+0.0	-0.0	-0.0
Pu-241	+0.0	-2.7	-2.7	+0.0	-0.0	-0.0
Pu-242	+0.0	-0.2	-0.2	+0.0	-0.0	-0.0
Am-241	+0.0	-0.1	-0.1	+0.0	-0.0	-0.0
Am-242m	+0.0	+0.0	+0.0	+0.0	+0.0	+0.0
Am-243	+0.0	+0.0	+0.0	+0.0	+0.0	+0.0
Cm-242	+0.0	+0.0	+0.0	+0.0	+0.0	+0.0
Cm-243	+0.0	+0.0	+0.0	+0.0	+0.0	+0.0
Cm-244	+0.0	+0.0	+0.0	+0.0	+0.0	+0.0
Cm-245	+0.0	+0.0	+0.0	+0.0	+0.0	+0.0
Total FP	+0.0	+7.3	+7.3	+0.0	+4.9	+4.9

Unit: kg

Remark: Reference of difference is result by JNC

Table 4.3-1(1) Comparison of the Keff in the best estimation benchmark - EGCR core -

Items	JNC	CEA	Discrepancy[*1]
Base value	0.99378	0.97873	-0.01505
Heterogeneity effect	-0.00041	+0.00440	+0.00481
Transport and mesh effect	+0.01666	+0.01780	+0.00114
Corrected value	1.01003	1.00093	-0.00910

*1: Reference is result by JNC.

Table 4.3-1(2) Comparison of the Keff in the best estimation benchmark - CPF core -

Items	JNC	CEA	Discrepancy[*1]
Base value	0.98305	0.97725	-0.00579
Heterogeneity effect	-0.00977	-0.00205	+0.00772
Transport and mesh effect	+0.02886	+0.01767	-0.01119
Corrected value	1.00214	0.99287	-0.00927

*1: Reference is result by JNC.

Table 4.3-2(1) Comparison in the Doppler effect in the best estimation benchmark
- EGCR core -

Items	JNC	CEA	Discrepancy*1 [factor]
Base value [10^{-3}Tdk/dT]	-3.55	-3.34	0.94
Heterogeneity effect [factor]	1.05 *2	1.07	1.02
Transport and mesh effect [factor]	1.00 *2	1.02	1.02
Corrected value [10^{-3}Tdk/dT]	-3.73	-3.65	0.98

*1: Reference is result by JNC.
*2: Typical value in JNC's design study

Table 4.3-2(2) Comparison in the Doppler effect in the best estimation benchmark
- CPF core -

Items	JNC	CEA	Discrepancy*1 [factor]
Base value [10^{-3}Tdk/dT]	-9.74	-9.93	1.02
Heterogeneity effect [factor]	1.05 *2	1.00	0.95
Transport and mesh effect [factor]	1.00 *2	1.02	1.02
Corrected value [10^{-3}Tdk/dT]	-10.23	-10.16	0.99

*1: Reference is result by JNC.
*2: Typical value in JNC's design study

Table 4.3-3(1) Comparison in the coolant depressurization reactivity in the best estimation benchmark - EGCR core -

Items	JNC	CEA	Discrepancy[*1]
Base value	+1.18	+1.31	+0.13
Heterogeneity effect	-0.11	-0.03	+0.08
Transport and mesh effect	+0.08	+0.05	-0.03
Corrected value	+1.15	+1.33	+0.18

Unit: $
*1: Reference is result by JNC.

Table 4.3-3(2) Comparison in the coolant depressurization reactivity in the best estimation benchmark - CPF core -

Items	JNC	CEA	Discrepancy[*1]
Base value	+1.28	+1.01	-0.27
Heterogeneity effect	-0.23	-0.01	+0.22
Transport and mesh effect	+0.32	+0.38	+0.06
Corrected value	+1.37	+1.38	+0.01

Unit: $
*1: Reference is result by JNC.

5. CONCLUSIONS

The GCFR neutronic benchmark has been performed within the NWP-2 (Innovative core and plant design) of the JNC/CEA bilateral agreement.

Basically results of core design parameters calculated by both CEA and JNC sides agree in a satisfactory manner and it is found that the discrepancies do not have a significant impact on the core conceptual design. Therefore results of this benchmark can be used for the proof of high design reliability in the core conceptual design characteristics by both JNC and CEA.

For improving the accuracy of the neutronic codes used for designing GCFR cores, this benchmark has been pointed out the following items:

(1) Criticality
Further investigations should be done particularly on the lumped FP cross-sections for core design and on heterogeneity effect, transport and mesh effects for the GCFR core designs.

(2) Burnup reactivity loss
Investigations on the FP cross-sections is required whatever the fast core design.

(3) Mass balance by depletion calculation
Investigation on many parameters such as the lumped FP weight, energy release per fission and consideration of the heat generation by non-fuel nuclides is required since with their discrepancies contribute to the mass differences between JNC and CEA.

These investigations are worth being investigated for improving the design accuracy of GCFR cores.

6. REFERENCES

(1) H. Noda and T. Inagaki: "Feasibility Study on Commercial FR Cycle Systems in Japan - The Results in the First Phase and Future Plants of the Study -", Proc. of Int. Conf. on: "Back-End of the Fuel Cycle: From Research to Solutions" GLOBAL 2001, Paris, France (2001).

(2) H. Hayashi, et al.: "Core Design Studies on Various Forms of Coolants and Fuel Materials (2) -Studies on Liquid Heavy Metal and Gas Cooled Cores, Small Cores and Evaluation of 4-type Cores -", JNC Technical Review, No.12 Extra Edition 2001.9, JNC TN1340 2001-008 (2001) [in Japanese].

(3) M. Naganuma, et al.: "Design Study on Core and Fuel Properties of Helium Gas Cooled Fast Reactors (Coated Particle Type Fuel Reactor / Pin Type Fuel Reactor) - Results in JFY2001 -", JNC TN9400 2002-074 (2002) [in Japanese].

(4) T. Hazama, et al.: "Development of the Unified Cross-section Set ADJ2000R for Fast Reactor Analysis", JNC TN9400 2002-064 (2002) [in Japanese].

(5) M. Nakagawa and K. Tsuchihashi: "SLAROM: A Code for Cell Homogenization Calculation of Fast Reactor", JAERI 1294 (1984).

(6) T. Mori and M. Nakagawa: "MVP/GMVP: General Purpose Monte Carlo Codes for Neutron and Photon Transport Calculations based on Continuous Energy and Multigroup Methods", JAERI-Data/Code 94-007 (1994) [in Japanese].

(7) E. Fort, et al.: "Realisation and Performance of the Adjusted Nuclear Data Library ERALIB1", Proc. of Int. Conf. on the Physics of Reactors (PHYSOR96), Session F03, Mito, Japan (1996).

(8) J. Y. Doriath, et al.: "ERANOS1: The Advanced European System of Codes for Reactor Physics Calculation", Int. Conf. on Mathematical Methods and Super Computing in Applications, Karlsruhe, Germany (1993).

(9) G.Rimpault, et al.: "Advanced Methods for Treating Heterogeneity and Streaming Effects in Gas Cooled Fast Reactors", Proc. Int. Conf. Mathematics and Computing (M&C'99), Madrid, Spain (1999).

(10) K. Sugino: "Evaluation on Neutronic Heterogeneity and Transport Effects of Gas-cooled Fast Reactor Cores", JNC TN9400 2002-050 (2002) [in Japanese].

7. ACKNOWLEDGMENT

The authors deeply appreciate the cooperation of A. Soga, H. Komoda and T. Iwai of the NESI Ltd. for GCFR core analyses.

A. APPENDIX

For two GCFR benchmarks, detailed data was compiled in the APPENDIX. The contents is as follows:

(1) 2D RZ core geometry data with thermal output
Fig. A.1-1 for the EGCR core
Fig. A.2-1 for the CPF core

(2) Homogeneous composition data of EOEC state for the base calculation benchmark with region-wise temperatures
Table A.1-1, A.1-2, A.1-3 for the EGCR core
Table A.2-1, A.2-2 for the CPF core

(3) Homogeneous fresh fuel composition data for the simple depletion calculation benchmark
Table A.1-4 for the EGCR core
Table A.2-3 for the CPF core

(4) Specification of the fuel subassembly for the best estimation benchmark
Table A.1-5 for the EGCR core
Table A.2-4, A.2-5 and Fig. A.2-2, A.2-3 for the CPF core

(5) Heterogeneous fresh fuel composition data for the best estimation benchmark
Table A.1-6 for the EGCR core
Table A.2-6 (Exact model), A.2-7 (Simplified model) for the CPF core

In the simplified model, fuel compartment region is smeared and the porosities of inner and outer ducts are taken into account.

Table A.1-1 Homogeneous fuel composition data at EOEC - EGCR core -

Nuclides	Inner Core [1]	Outer Core [2]	Lower Axial Blanket [3]	Upper Axial Blanket [4]	Radial Blanket
Pu-238	1.66064E-05	2.25714E-05	1.47757E-07	7.21652E-08	6.78929E-08
Pu-239	5.87890E-04	7.16094E-04	2.45582E-04	1.65263E-04	1.97657E-04
Pu-240	3.83894E-04	5.24373E-04	1.93531E-05	7.82521E-06	9.36755E-06
Pu-241	5.32468E-05	7.06342E-05	9.37672E-07	2.39959E-07	3.14512E-07
Pu-242	4.45512E-05	6.26592E-05	3.52287E-08	6.30383E-09	8.90821E-09
U-235	7.25521E-06	7.05254E-06	1.37980E-05	1.61895E-05	2.62059E-05
U-236	1.38110E-06	1.10854E-06	1.53978E-06	9.98101E-07	1.27162E-06
U-238	4.30044E-03	3.88876E-03	6.45358E-03	6.58113E-03	1.01531E-02
Am-241	2.45253E-05	3.62785E-05	9.15020E-08	2.44155E-08	3.28244E-08
Am-242m	1.43319E-06	1.85504E-06	1.89293E-09	3.58902E-10	5.23117E-10
Am-243	1.23618E-05	1.72655E-05	1.21502E-09	1.50723E-10	2.42794E-10
Np-237	5.37702E-06	7.15425E-06	7.67716E-07	5.65766E-07	5.01936E-07
Np-239	5.97310E-07	4.43365E-07	5.03297E-07	3.05581E-07	3.56811E-07
Cm-242	1.08916E-06	1.30394E-06	2.36569E-09	4.26143E-10	6.06332E-10
Cm-243	8.76175E-08	9.46192E-08	7.16472E-11	9.19755E-12	1.48960E-11
Cm-244	1.34310E-05	1.83762E-05	1.12204E-10	1.00805E-11	1.85294E-11
Cm-245	1.63318E-06	2.00319E-06	3.66715E-12	2.42040E-13	5.08920E-13
O-16	1.26023E-02	1.26387E-02	1.41237E-02	1.41237E-02	2.11699E-02
C-12	2.45965E-04	2.45965E-04	2.45965E-04	2.45965E-04	1.53363E-04
Fe	8.42069E-03	8.42068E-03	8.42069E-03	8.42069E-03	1.04777E-02
Cr	2.23255E-03	2.23254E-03	2.23254E-03	2.23254E-03	2.77789E-03
Ni	2.56274E-03	2.56273E-03	2.56273E-03	2.56273E-03	3.18875E-03
Mo	2.01794E-04	2.01793E-04	2.01793E-04	2.01793E-04	2.51085E-04
Mn	2.76583E-04	2.76583E-04	2.76583E-04	2.76583E-04	3.44145E-04
FP-U238	7.24951E-05	6.94862E-05	2.44963E-05	1.77598E-05	1.54539E-05
FP-Pu239	3.73179E-04	4.42547E-04	4.33460E-05	1.94266E-05	2.03231E-05
FP-U235	6.07631E-06	4.97637E-06	5.46083E-06	3.56453E-06	4.25961E-06
FP-Pu241	1.15836E-04	1.54402E-04	5.68362E-07	1.74482E-07	1.84175E-07
Nd-143	1.97136E-04	1.97136E-04			
B-10					
B-11					

Unit: $10^{24}/cm^3$

Table A.1-2 Homogeneous non-fuel composition data - EGCR core -

Nuclides	Gas Plenum [6]	Upper Axial Shield [7]	Radial Shield [8]	Rod Follower [9]	Control Rod [10]
Pu-238					
Pu-239					
Pu-240					
Pu-241					
Pu-242					
U-235					
U-236					
U-238					
Am-241					
Am-242m					
Am-243					
Np-237					
Np-239					
Cm-242					
Cm-243					
Cm-244					
Cm-245					
O-16	4.86099E-04	2.72239E-04	2.78378E-04	8.74491E-04	4.44222E-04
C-12	2.43049E-04	1.32910E-02	1.39189E-04	4.37246E-04	7.28890E-03
Fe	7.49810E-03	9.12047E-03	3.93331E-02	3.23581E-03	9.01397E-03
Cr	2.51480E-03	2.55025E-03	1.09982E-02	9.04790E-04	2.38984E-03
Ni	3.38440E-03	1.79421E-03	7.73774E-03	6.36560E-04	2.74328E-03
Mo	2.28780E-04	2.03256E-04	8.76566E-04	7.21124E-05	2.16010E-03
Mn	1.50180E-04	2.41368E-04	1.04093E-03	8.56339E-05	2.96069E-03
FP-U238					
FP-Pu239					
FP-U235					
FP-Pu241					
Nd-143					
B-10		1.04540E-02			2.30330E-02
B-11		4.21655E-02			5.23470E-03

Unit: $10^{24}/cm^3$

Table A.1-3　Region-wise temperature data　-EGCR core -

Region	Temperature [^{o}C]
[1]　Inner core	1227
[2]　Outer core	1227
[3]　Lower axial blanket	630
[4]　Upper axial blanket	630
[5]　Radial blanket	630
[6]　Gas plenum	380
[7]　Upper axial shield	380
[8]　Radial Shield	380
[9]　Rod follower	380
[10]　Control rod	380

Table A.1-4　Homogeneous fresh fuel composition data　- EGCR core -

Nuclides	Inner Core [1]	Outer Core [2]	Lower Axial Blanket [3]	Upper Axial Blanket [4]	Radial Blanket
Pu-238	1.37492E-05	1.95129E-05			
Pu-239	6.73376E-04	9.55653E-04			
Pu-240	3.97878E-04	5.64668E-04			
Pu-241	5.30766E-05	7.53262E-05			
Pu-242	4.79402E-05	6.80366E-05			
U-235	1.45087E-05	1.29833E-05	2.07084E-05	2.07084E-05	3.16940E-05
U-236					
U-238	4.76081E-03	4.26029E-03	6.79515E-03	6.79515E-03	1.03999E-02
Am-241	2.47101E-05	3.50686E-05			
Am-242m					
Am-243	1.22541E-05	1.73910E-05			
Np-237	6.28247E-06	8.91608E-06			
Np-239					
Cm-242					
Cm-243					
Cm-244	1.22038E-05	1.73196E-05			
Cm-245					
O-16	1.26023E-02	1.26387E-02	1.41237E-02	1.41237E-02	2.11699E-02
C-12	2.45965E-04	2.45965E-04	2.45965E-04	2.45965E-04	1.53363E-04
Fe	8.42069E-03	8.42068E-03	8.42069E-03	8.42069E-03	1.04777E-02
Cr	2.23255E-03	2.23254E-03	2.23254E-03	2.23254E-03	2.77789E-03
Ni	2.56274E-03	2.56273E-03	2.56273E-03	2.56273E-03	3.18875E-03
Mo	2.01794E-04	2.01793E-04	2.01793E-04	2.01793E-04	2.51085E-04
Mn	2.76583E-04	2.76583E-04	2.76583E-04	2.76583E-04	3.44145E-04
FP-U238					
FP-Pu239					
FP-U235					
FP-Pu241					
Nd-143	1.97136E-04	1.97136E-04			
B-10					
B-11					

Unit: $10^{24}/cm^3$

Table A.1-5 Specification of the fuel subassembly - EGCR core -

	Core	Axial blanket	Radial blanket
Core material	SS 316 *1	←	←
Fuel pin outer diameter (mm)	7.29	←	10.86
Fuel pin inner diameter (mm)	6.45	←	9.66
Clad thickness (mm)	0.42	←	0.60
Fuel smeared density (%TD)	82	91.4	←
Number of fuel pins in S/A	397	←	271
Wrapper tube thickness (mm)	4.4	←	←
Wrapper tube outer flat to flat (mm)	216.57	←	←
Fuel subassembly gap (mm)	5.0	←	←
Fuel subassembly pitch (mm)	221.57	←	←
Fuel volume fraction (%) *2	30.5	←	46.7
Structure volume fraction (%)	16.1	←	20.0
Coolant volume fraction (%)	53.4	←	33.3

*1 Fe / Cr / Ni / Mo / Mn = 60.97 / 15.05 / 19.5 / 2.51 / 1.97 (wt%)

*2 the area of inside the cladding

Table A.1-6 Heterogeneous fresh fuel composition data - EGCR core -

Fuel Pellet

Nuclides	Inner Core [1]	Outer Core [2]	Lower Axial Blanket [3]	Upper Axial Blanket [4]	Radial Blanket
Pu-238	4.50646E-05	6.39558E-05			
Pu-239	2.20707E-03	3.13226E-03			
Pu-240	1.30409E-03	1.85076E-03			
Pu-241	1.73965E-04	2.46890E-04			
Pu-242	1.57129E-04	2.22998E-04			
U-235	4.75539E-05	4.25542E-05	6.78741E-05	6.78741E-05	6.78731E-05
U-236					
U-238	1.56041E-02	1.39636E-02	2.22719E-02	2.22719E-02	2.22715E-02
Am-241	8.09902E-05	1.14941E-04			
Am-242m					
Am-243	4.01642E-05	5.70010E-05			
Np-237	2.05915E-05	2.92235E-05			
Np-239					
Cm-242					
Cm-243					
Cm-244	3.99993E-05	5.67670E-05			
Cm-245					
FP-U238					
FP-Pu239					
FP-U235					
FP-Pu241					
Nd-143	6.46136E-04	6.46136E-04			
O-16	3.96931E-02	3.98124E-02	4.46797E-02	4.46797E-02	4.46787E-02

Structure Material

Nuclides	Common
Fe	5.23978E-02
Cr	1.38921E-02
Ni	1.59467E-02
Mo	1.25566E-03
Mn	1.72104E-03

Coolant

Nuclides	Common
O-16	9.20872E-04
C-12	4.60436E-04

Unit: $10^{24}/cm^3$

Table A.2-1 Homogeneous fuel composition data at EOEC - CPF core -

Region	Inner core	Outer core	R-blanket	A-blanket
Temperature [K]	1030	1030	930	930
Pu-238	1.30763E-05	1.62358E-05	3.44855E-08	2.12251E-07
Pu-239	4.89521E-04	5.90538E-04	1.05852E-04	1.59425E-04
Pu-240	2.95902E-04	3.80546E-04	5.87433E-06	1.52379E-05
Pu-241	4.18429E-05	4.92267E-05	6.14165E-07	4.07492E-06
Pu-242	3.38052E-05	4.45048E-05	3.16560E-08	5.65756E-07
Am-241	1.98868E-05	2.90007E-05	7.28792E-08	4.62935E-07
Am-242m	1.13642E-06	1.20031E-06	1.23338E-09	1.38662E-08
Am-243	9.29642E-06	1.20425E-05	1.00270E-09	5.22285E-08
Cm-242	7.48891E-07	6.98342E-07	1.72286E-09	2.74268E-08
Cm-243	6.17615E-08	4.26291E-08	2.58825E-11	1.01916E-09
Cm-244	1.00749E-05	1.26573E-05	6.49867E-11	1.08231E-08
Cm-245	1.22373E-06	1.13804E-06	1.06893E-12	4.66769E-10
U-235	7.28496E-06	8.15510E-06	2.13298E-05	1.42731E-05
U-236	1.16461E-06	8.16008E-07	1.05932E-06	1.59513E-06
U-238	3.90001E-03	3.73423E-03	8.46573E-03	6.92926E-03
Np-237	3.94746E-06	5.22391E-06	2.97275E-07	6.21599E-07
Np-239	4.08546E-07	2.56795E-07	1.87070E-07	3.37935E-07
N-15	1.25255E-02	1.25255E-02	1.50620E-02	1.25690E-02
N-14				
He-4	2.57185E-04	2.57185E-04	2.59000E-04	2.94999E-04
U-235 Lumped FP	4.49364E-06	3.08542E-06	3.84560E-06	6.06961E-06
U-238 Lumped FP	4.51681E-05	3.36372E-05	8.64797E-06	1.88816E-05
Pu-239 Lumped FP	2.14710E-04	1.82715E-04	1.25030E-05	4.14277E-05
Pu-241 Lumped FP	5.84518E-05	5.26846E-05	1.23201E-07	1.91171E-06
Cr-natural				
Fe-natural				
Ni-natural				
Mo-natural				
B-10				
B-11				
C-12	3.84560E-03	3.84560E-03	3.84600E-03	3.84600E-03
O-16				
Si-natural	3.84560E-03	3.84560E-03	3.84600E-03	3.84600E-03
Ti-natural	7.42416E-03	7.42415E-03	6.43499E-03	5.36999E-03
Zr-natural				
W-natural				
FP (Nd-143)	1.39538E-04	1.39538E-04		

R-: Radial A-: Axial

Unit: $10^{24}/cm^3$

Table A.2-2 Homogeneous non-fuel composition data - CPF core -

Region	R-shield	A-shield	C-follower	C-reflector
Temperature [K]	773	773	773	773
Pu-238				
Pu-239				
Pu-240				
Pu-241				
Pu-242				
Am-241				
Am-242m				
Am-243				
Cm-242				
Cm-243				
Cm-244				
Cm-245				
U-235				
U-236				
U-238				
Np-237				
Np-239				
N-15				
N-14				
He-4	2.26000E-05	1.35480E-04	4.29000E-04	4.51600E-05
U-235 Lumped FP				
U-238 Lumped FP				
Pu-239 Lumped FP				
Pu-241 Lumped FP				
Cr-natural				
Fe-natural				
Ni-natural				
Mo-natural				
B-10				
B-11				
C-12	1.07250E-01	7.90300E-02	2.40300E-03	1.01610E-01
O-16				
Si-natural				
Ti-natural				
Zr-natural				
W-natural				
FP (Nd-143)				

R-: Radial A-: Axial C-: Control rod

Unit: $10^{24}/cm^3$

Table A.2-3 Homogeneous fresh fuel composition data - CPF core -

Region	Inner core	Outer core	R-blanket	A-blanket
Temperature [K]	1030	1030	930	930
Pu-238	1.01350E-05	1.33270E-05		
Pu-239	4.96360E-04	6.52710E-04		
Pu-240	2.93280E-04	3.85670E-04		
Pu-241	3.91240E-05	5.14480E-05		
Pu-242	3.53370E-05	4.64690E-05		
Am-241	1.81970E-05	2.39290E-05		
Am-243	9.02380E-06	1.18660E-05		
Cm-243				
Cm-244	8.98680E-06	1.18180E-05		
Cm-245				
U-235	1.29220E-05	1.20630E-05	2.62120E-05	2.18729E-05
U-236				
U-238	4.24020E-03	3.95820E-03	8.60108E-03	7.17728E-03
Np-237	4.62610E-06	6.08340E-06		
N-15	1.25670E-02	1.25670E-02	1.50620E-02	1.25690E-02
N-14				
He-4	2.57000E-04	2.57000E-04	2.59000E-04	2.95000E-04
Cr-natural				
Fe-natural				
Ni-natural				
Mo-natural				
B-10				
B-11				
C-12	3.84600E-03	3.84600E-03	3.84600E-03	3.84600E-03
O-16				
Si-natural	3.84600E-03	3.84600E-03	3.84600E-03	3.84600E-03
Ti-natural	7.42300E-03	7.42300E-03	6.43500E-03	5.37000E-03
Zr-natural				
W-natural				
FP (Nd-143)	1.40000E-04	1.40000E-04		

R-: Radial A-: Axial

Unit: $10^{24}/cm^3$

Table A.2-4(1) Specification of coated-particle fuel (Core region) - CPF core -

Region	Specification	Volume fraction
Kernel	Radius: 0.75mm	0.16255
Low density (inner) TiN layer	Thickness: 0.12mm	0.09117
High density (outer) TiN layer	Thickness: 0.10mm	0.09793
Particle fuel (Sum)	Radius: 0.97mm	0.35166
Packing density	60%	-

Remark: High melting point coating metal was not considered

Table A.2-4(2) Specification of coated-particle fuel (Axial blanket region) - CPF core -

Region	Specification	Volume fraction
Kernel	Radius: 0.85mm	0.22257
Low density (inner) TiN layer	Thickness: 0.06mm	0.05054
High density (outer) TiN layer	Thickness: 0.08mm	0.07855
Particle fuel (Sum)	Radius: 0.99mm	0.35166
Packing density	60%	-

Remark: High melting point coating metal was not considered

Table A.2-5 Specification of fuel subassembly - CPF core -

Region	Specification	Volume fraction
Porous inner firt	Inner radius: 42mm Outer radius: 46mm Porosity: 5%	- - -
Porous outer frit	Inner radius: 100.5mm Outer radius: 104.5mm Porosity: 40%	- - -
Supporter *(Assumed to be a hexagonal tube)*	Inner flat to flat: 215mm Outer flat to flat: 221mm *Porosity: 63%*	- - -
Structure total (SiC)	-	0.08025
Coolant (He)	-	0.56809
SA pitch	222.3mm	-
Core height	1,800mm	-
Axial blanket height	400mm (Lower and upper)	-
Axial shield height	500mm (Lower and upper)	-

Table A.2-6(1) Heterogeneous fresh fuel composition data for the exact model (Inner core) - CPF core -

Region	Coated-particle fuel			Coolant	Structure
Part	Kernel	Inner TiN	Outer TiN	He	SiC
Temperature [K]	1030	1030	1030	1030	1030
Pu-238	6.23494E-05				
Pu-239	3.05355E-03				
Pu-240	1.80423E-03				
Pu-241	2.40686E-04				
Pu-242	2.17389E-04				
Am-241	1.11946E-04				
Am-243	5.55134E-05				
Cm-243					
Cm-244	5.52858E-05				
Cm-255					
U-235	7.94947E-05				
U-236					
U-238	2.60852E-02				
Np-237	2.84593E-05				
N-15	3.14870E-02	2.59500E-02	5.19000E-02		
N-14					
He-4				4.51600E-04	
Cr-natural					
Fe-natural					
Ni-natural					
Mo-natural					
B-10					
B-11					
C-12					4.80700E-02
O-16					
Si-natural					4.80700E-02
Ti-natural		2.59500E-02	5.19000E-02		
Zr-natural					
W-natural					
FP (Nd-143)	8.61264E-04				

Unit: $10^{24}/cm^3$

Table A.2-6(2) Heterogeneous fresh fuel composition data for exact model (Outer core) - CPF core -

Region	Coated-particle fuel			Coolant	Structure
Part	Kernel	Inner TiN	Outer TiN	He	SiC
Temperature [K]	1030	1030	1030	1030	1030
Pu-238	8.19862E-05				
Pu-239	4.01540E-03				
Pu-240	2.37260E-03				
Pu-241	3.16502E-04				
Pu-242	2.85872E-04				
Am-241	1.47209E-04				
Am-243	7.29983E-05				
Cm-243					
Cm-244	7.27030E-05				
Cm-255					
U-235	7.42102E-05				
U-236					
U-238	2.43504E-02				
Np-237	3.74244E-05				
N-15	3.14870E-02	2.59500E-02	5.19000E-02		
N-14					
He-4				4.51600E-04	
Cr-natural					
Fe-natural					
Ni-natural					
Mo-natural					
B-10					
B-11					
C-12					4.80700E-02
O-16					
Si-natural					4.80700E-02
Ti-natural		2.59500E-02	5.19000E-02		
Zr-natural					
W-natural					
FP (Nd-143)	8.61264E-04				

Unit: $10^{24}/cm^3$

Table A.2-6(3) Heterogeneous fresh fuel composition data for exact model (Axial blanket) - CPF core -

Region	Coated-particle fuel			Coolant	Structure
Part	Kernel	Inner TiN	Outer TiN	He	SiC
Temperature [K]	930	930	930	930	930
Pu-238					
Pu-239					
Pu-240					
Pu-241					
Pu-242					
Am-241					
Am-243					
Cm-243					
Cm-244					
Cm-255					
U-235	9.82725E-05				
U-236					
U-238	3.22467E-02				
Np-237					
N-15	3.22630E-02	2.59500E-02	5.19000E-02		
N-14					
He-4				5.17500E-04	
Cr-natural					
Fe-natural					
Ni-natural					
Mo-natural					
B-10					
B-11					
C-12					4.80700E-02
O-16					
Si-natural					4.80700E-02
Ti-natural		2.59500E-02	5.19000E-02		
Zr-natural					
W-natural					
FP (Nd-143)					

Unit: $10^{24}/cm^3$

Table A.2-7(1) Heterogeneous fresh fuel composition data for the simplified model (Inner core) - CPF core -

Region	Smeared Fuel	Inner tube	Outer tube	Supporter	Coolant
Temperature [K]	1030	1030	1030	1030	1030
Pu-238	1.72923E-05				
Pu-239	8.46886E-04				
Pu-240	5.00392E-04				
Pu-241	6.67531E-05				
Pu-242	6.02918E-05				
Am-241	3.10476E-05				
Am-243	1.53963E-05				
Cm-243					
Cm-244	1.53332E-05				
Cm-255					
U-235	2.20474E-05				
U-236					
U-238	7.23460E-03				
Np-237	7.89302E-06				
N-15	2.14417E-02				
N-14					
He-4	1.80640E-04	2.25800E-05	1.80640E-04	2.84508E-04	4.51600E-04
Cr-natural					
Fe-natural					
Ni-natural					
Mo-natural					
B-10					
B-11					
C-12		4.56665E-02	2.88420E-02	1.77859E-02	
O-16					
Si-natural		4.56665E-02	2.88420E-02	1.77859E-02	
Ti-natural	1.27090E-02				
Zr-natural					
W-natural					
FP (Nd-143)	2.38867E-04				

Unit: $10^{24}/cm^3$

Table A.2-7(2) Heterogeneous fresh fuel composition data for the simplified model (Outer core) - CPF core -

Region	Smeared Fuel	Inner tube	Outer tube	Supporter	Coolant
Temperature [K]	1030	1030	1030	1030	1030
Pu-238	2.27384E-05				
Pu-239	1.11365E-03				
Pu-240	6.58028E-04				
Pu-241	8.77802E-05				
Pu-242	7.92851E-05				
Am-241	4.08275E-05				
Am-243	2.02457E-05				
Cm-243					
Cm-244	2.01638E-05				
Cm-255					
U-235	2.05818E-05				
U-236					
U-238	6.75346E-03				
Np-237	1.03795E-05				
N-15	2.14417E-02				
N-14					
He-4	1.80640E-04	2.25800E-05	1.80640E-04	2.84508E-04	4.51600E-04
Cr-natural					
Fe-natural					
Ni-natural					
Mo-natural					
B-10					
B-11					
C-12		4.56665E-02	2.88420E-02	1.77859E-02	
O-16					
Si-natural		4.56665E-02	2.88420E-02	1.77859E-02	
Ti-natural	1.27090E-02				
Zr-natural					
W-natural					
FP (Nd-143)	2.38867E-04				

Unit: $10^{24}/cm^3$

Table A.2-7(3) Heterogeneous fresh fuel composition data for the simplified model (Axial blanket) - CPF core -

Region	Smeared fuel	Inner tube	Outer tube	Supporter	Coolant
Temperature [K]	930	930	930	930	930
Pu-238					
Pu-239					
Pu-240					
Pu-241					
Pu-242					
Am-241					
Am-243					
Cm-243					
Cm-244					
Cm-255					
U-235	3.73194E-05				
U-236					
U-238	1.22458E-02				
Np-237					
N-15	2.14451E-02				
N-14					
He-4	2.07000E-04	2.58750E-05	2.07000E-04	3.26025E-04	5.17500E-04
Cr-natural					
Fe-natural					
Ni-natural					
Mo-natural					
B-10					
B-11					
C-12		4.56665E-02	2.88420E-02	1.77859E-02	
O-16					
Si-natural		4.56665E-02	2.88420E-02	1.77859E-02	
Ti-natural	9.19313E-03				
Zr-natural					
W-natural					
FP (Nd-143)					

Unit: $10^{24}/cm^3$

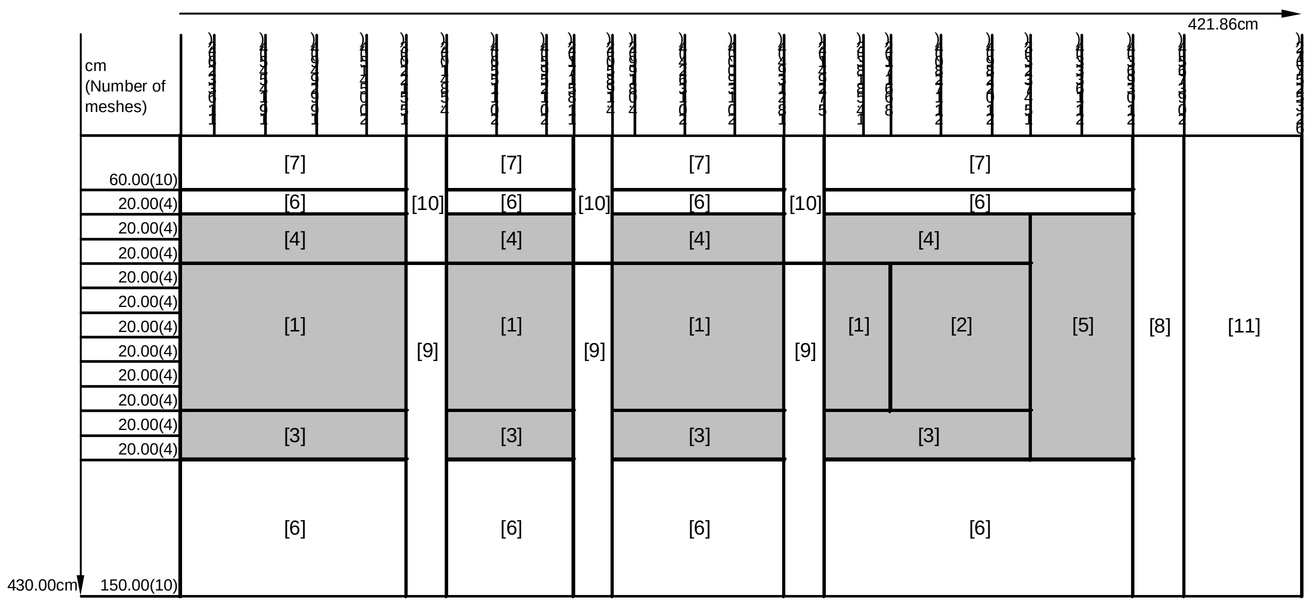

[1] inner core (Homogeneous and heterogeneous models)
[2] outer core (Homogeneous and heterogeneous models)
[3] lower axial blanket (Homogeneous and heterogeneous models)
[4] upper axial blanket (Homogeneous and heterogeneous models)
[5] radial blanket (Homogeneous and heterogeneous models)
[6] gas plenum (Homogeneous model only)
[7] upper axial shield (Homogeneous model only)
[8] SS radial shield (Homogeneous model only)
[9] CR follower (Homogeneous model only)
[10] Control rod (Homogeneous model only)
[11] B4C radial shield (Homogeneous model only)

Thermal output: 3,600MWt

Fig. A.1-1 Two-dimensional RZ core calculation model -EGCR core -

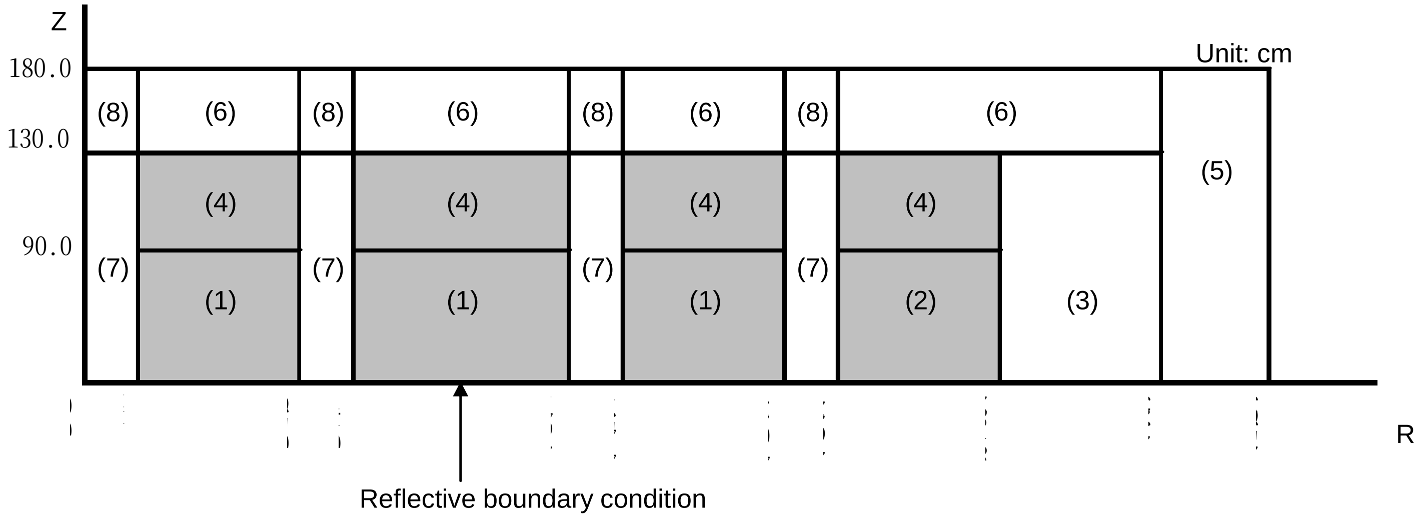

(1) Inner core (Homogeneous and heterogeneous models)
(2) Outer core (Homogeneous and heterogeneous models)
(3) Radial blanket (Homogeneous model only)
(4) Axial blanket (Homogeneous and heterogeneous models)
(5) Radial shield (Homogeneous model only)
(6) Axial shield (Homogeneous model only)
(7) Control rod follower (Homogeneous model only)
(8) Control rod reflector (Homogeneous model only)

Thermal output: 2,400MWt

Fig. A.2-1 Two-dimensional RZ core calculation model -CPF core -

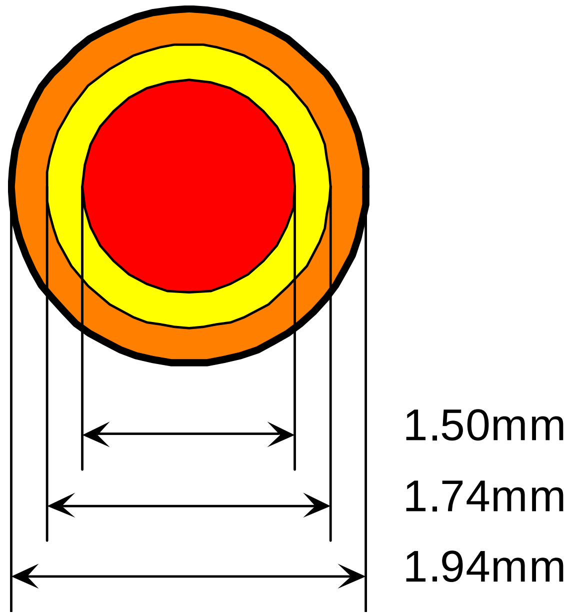

Fig. A.2-2 Configuration of the coated-particle fuel of core region (Example) -CPF core -

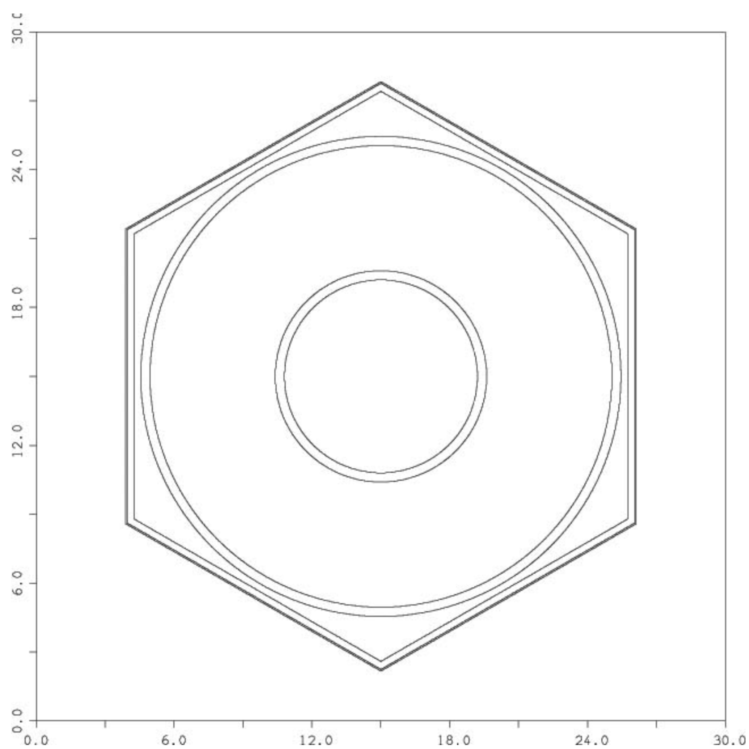

Fig. A.2-3 Cross-sectional view of the fuel subassembly in fuel part -CPF core -